European Review for Medical and Pharmacological Sciences 2022; 26: 1183-1195

Pharmacokinetics of HupA-PLGA-NPs of different sizes in the mouse blood and brain determined by LC-MS/MS

R.-H. ZHANG, C. WANG, T. SHI, X.-J. CHEN, J.-F. XU, M. SHI, L.-Q. LI

State Key Laboratory of NBC Protection for Civilian, Beijing, China

Abstract. – OBJECTIVE: Huperzine A, which was extracted from a Chinese herb, is a reversible and selective inhibitor of acetylcholinesterase (AChE), which is used as an anti-Alzheimer's drug that exerts evident pretreatment effects against exposure to organophosphate chemical warfare agents or pesticides. The aims of this study were to establish an LC-MS/MS method for the detection of HupA in biological samples and to investigate the pharmacokinetics of HupA polylactic-co-glycolic acid nanoparticles (HupA-PLGA-NPs) with different diameters in mice.

MATERIALS AND METHODS: The proposed LC-MS/MS method was established by optimizing the MS conditions and validating the specificity, linear range, lower limit, precision, accuracy, matrix effects, absolute recovery, and sample stability of the method. ICR mice were divided into three treatment groups: the HupA control group, the 46.4-nm HupA-PLGA-NP group and the 208.5-nm HupA-PLGA-NP group. All the mice in the three groups were administered 0.5 mg/kg HupA *via* the tail vein. The pharmacokinetic parameters in plasma and the brain were detected by LC-MS/MS. Pharmacokinetic parameters were analyzed using PKS pharmacokinetic software, and the relative bioavailability and brain-targeted drug targeting efficiency (DTE) were also calculated.

RESULTS: The distributions of HupA-PLGA-NP groups showed marked changes compared with that of HupA in mice *in vivo*, and the particle size of nanodrugs exerted a significant effect on the pharmacokinetic parameters in mice. The half-life ($T_{1/2}$) values in plasma of the 46.4- and 208.5-nm HupA-PLGA-NPs were 1.53- and 1.96-fold longer than that of the HupA at the same dose. The bioavailabilities of the two nanoparticles were 1.93- and 2.19-fold higher than that of HupA, respectively. In the brain, the T_{max} values of the two HupA-PLGA-NPs of different sizes was 1.25 h, which was clearly longer than that of HupA (0.5 h), and the corresponding $T_{1/2}$ values were 12.53 h and 8.47 h, which were 1.82- and 1.23-fold higher than that of HupA (6.89 h). In addition, the brain targeting index of the 46.40-nm HupA-PLGA-NPs was 1.48, which revealed an evident brain-targeting effect.

CONCLUSIONS: The LC-MS/MS method has the advantages of good specificity, high sensitivity and needing a low sample amount and is economical and particularly suitable for determining the drug content in plasma and brain samples. The NP size is associated with the distribution patterns of nanodrugs. Therefore, a particular NP size can be selected to maximize the pharmacodynamics effects and control the toxicity of nanodrugs.

Key Words:
Huperzine A, Nanoparticles, PLGA, Pharmacokinetics.

Introduction

Huperzine A (HupA), which was extracted from the Chinese herb *Huperzia serrata*[1], has been found to be an efficient, reversible, and highly selective inhibitor of AChE[2]. HupA can target sites of AChE and thereby significantly increases the concentration of acetylcholine in the brain, which has been proven to be effective in treating Alzheimer's disease[3,4]. Furthermore, it has been demonstrated that HupA can significantly reduce nerve agent lethality by reversibly inhibiting AChE in the blood and brain.

Nanodrug delivery systems (NDDs) are produced by the application of nanotechnology and nanocarrier materials in the field of pharmacy. Nanocarriers mainly include NPs, nanomicelles, nanoemulsions and liposomes[5]. Recent studies[6,7] have found that compared with other nanocarriers, NPs have the advantages of prolonging a drug's biological half-life, improving bioavailability and efficacy, reducing the nonspecific cell uptake and side effects of a drug and reducing the frequency of drug administration. Polycarbonate alkanes, high-molecular-weight polymers, and human serum albumin (HSA) are the three categories of biocompatible and biodegradable nanocarrier materials for brain-targeted NPs that are most

Corresponding Author: Liqin Li, MD; e-mail: llq969696@126.com

commonly used in brain-targeted studies[8]. Among them, PLGA, a type of high-molecular-weight polymer approved for Phase II clinical trials by the US Food and Drug Administration (FDA) and the European Medical Administration (EMA), is widely used as a nanocarrier material for NDDs. Based on its advantages of nontoxicity, non-immunogenicity, reproducibility of physicochemical properties and predictability, PLGA plays an increasingly important role in the search for new drug preparations.

The nanoparticle size is one of the most important parameters for the intracellular localization of NPs, as well as for NP transport across the blood-brain barrier[9]. For example, some research suggests that the NPs with a diameter of approximately 50 nm can more easily be internalized into endothelial cells through receptor-mediated endocytosis than NPs of other sizes[10,11]. In a previous study[12], 208.5-nm HupA-PLGA-NPs showed lower toxicity than HupA in mice and exhibited effective protection against the nerve agent soman poison for a longer time. A subsequent study proved that HupA-PLGA-NPs of different sizes show evident differences in toxic effects and effective protective times against the nerve agent soman poison. However, little is known about the pharmacokinetics of NPs with different particle sizes. Therefore, in our study, we aimed to establish an LC-MS/MS method for the determination of HupA in the plasma and brain of mice and to study the pharmacokinetics of HupA-PLGA-NPs of different sizes in the blood and brain. By comparing the pharmacokinetic parameters of HupA with those of HupA-PLGA-NPs in the blood and brain, we can understand the *in vivo* distribution characteristics and brain-targeting drug delivery characteristics. These results could provide a technical basis for the feasibility of the application of HupA-PLGA-NPs of different sizes.

Materials and Methods

Experimental Apparatus

The experimental apparatuses used in our study were as follows: Agilent 1200/6410 LC/QQQ system (Agilent, Santa Clara, CA, USA); Genie Vortex 2 Vortex oscillator (Scientific Industries, New York, NY, USA); Sigma 1-14 high-speed centrifuge (Sigma Corporation, St. Louis, MO, USA); N-EVAP nitrogen blower (Organonation, Berlin, MA, USA); Sartorius BT-25S analytical balance (Sartorius, Göttingen, Germany); Purelab Plus pure water meter (Pall, New York, NY, USA); and KQ2200 ultrasonic cleaner (Kunshan Ultrasonic Instrument Co., LTD., Kunshan, China).

Chemicals and Reagents

First, 46.4- and 208.5-nm HupA-PLGA-NPs were prepared by our research group. HupA (purity≥98.0%) and HupB (purity≥98.0%, IS) were provided by Yifang Technology Co., Ltd. (Tianjin, China). LC/MS-grade methanol, methanoic acid and ethyl acetate were purchased from Sigma-Aldrich (St. Louis, MO, USA). All other chemical agents in this study were of analytical grade. Ultrapure water was freshly purified using an ultra-pure water purifier system.

LC-MS/MS Conditions

Chromatographic separation was carried out using an XDB-C18 column (100×2.1 mm, 3.5 μm). The mobile phase consisted of methanol and 0.2% formic acid water (50/50, V/V) and was applied at a flow rate of 0.2 mL/min, and the injection volume was consistently 10 μL. The column temperature was kept at 25°C.

Sample ionization was achieved by electrospray in the positive ion mode (ESI), and subsequent quantitative analysis was performed using the MRM mode with the target fragment ions m/z 243.1→226.1 for HupA and m/z 257.2→240.1 for HupB (IS). The optimized ionization monitoring conditions were set as follows: capillary voltage of 5.0 kV, fragmentor voltage of 135 V, and high-purity nitrogen gas as the desolvation gas (9 L/min) at 300°C.

Preparation of Calibration Solutions and Quality Control (QC) Samples

The primary stock solutions of HupA and IS were prepared at a concentration of 1.0 mg/mL in methanol and then stored at 4°C. A series of concentrations of standard working solution and 100 ng/mL IS working solution were prepared with the HupA and IS stock solutions, respectively, and diluted with methanol and 0.2% formic acid water (50/50). Calibration standards were obtained by mixing blank mouse plasma with the corresponding standard working solution to achieve final sample concentrations of 0.1, 0.25, 0.5, 1.0, 2.5, 5.0, 10, 25, 50, and 100 ng/mL. Similarly, the QC samples were individually prepared at three different concentration levels of 0.25, 5, and 80 ng/

mL. The brain tissue homogenate calibration standards were obtained using an approach similar to that used for the plasma samples. The quantitative lower limit was investigated with a concentration of 0.1 ng/mL.

Sample Preparation

HupA and IS were extracted from blood or brain tissues using a one-step protein precipitation approach. Briefly, 200 μL of plasma or brain tissue homogenates was transferred to a 1.5-mL Eppendorf tube, and 10 μL of IS (100 ng/mL), 10 μL of NaOH (pH 11.0) and 1 mL of ethyl acetate were then added. The mixture solutions were vortexed for 3 min and then centrifuged at 12,000 rpm for 10 min. The upper organic phase was transferred to another Eppendorf tube and dried under nitrogen at 50°C, and the residue was dissolved in 200 μL of the mobile phase and centrifuged at 120,00 rpm for 10 min. Subsequently, 160 μL of supernatant was collected for analysis.

Specificity Analysis

Two hundred microliters of plasma and brain tissue samples without IS were used as the blank control and processed and analyzed according to Section sample preparation. The chromatograms of the blank control plasma sample was obtained and designated A. The HupA standard solution and the HupB working solution (IS) were precisely absorbed and added to the blank plasma and brain tissue samples to obtain final HupA and IS concentrations of 0.1 and 5 ng/mL, respectively. The samples were processed and analyzed according to the steps used for sample processing. The chromatogram of the plasma samples with the standard samples was obtained and designated B. The plasma samples from the mice after drug administration were processed and analyzed as described above, and the chromatogram was obtained and designated C. The chromatograms A, B, and C were compared to investigate the specificity of the method.

Preparation of Sample Standard Curves

A series of standard working solution of the plasma and brain homogenate samples of HupA at concentrations of 0.1, 0.25, 0.5, 1, 2.5, 5, 10, 25, 50, and 100 ng/mL were pretreated using a one-step protein precipitation approach and analyzed by LC-MS/MS. The drug concentration was plotted by comparing the measured HupA peak area with the HupB peak area, and the standard curve equation of the plasma and tissue samples was obtained through regression analysis with the least-square method.

Precision and Accuracy Analyses

Blank plasma and brain tissue homogenates of mice were used to prepare quality control (QC) samples with low, medium, and high concentrations (0.25, 5 and 80 ng/mL, respectively). The sample with each concentration was measured five times a day for 5 consecutive days. The intraday and interday precision and accuracy of IS were similarly evaluated. The accuracy was determined as a percentage calculated based on the deviation of the measured mean drug concentration to the theoretical drug concentration value. The precision was expressed by the relative standard precision (RSD).

Analyses of the Matrix Effect and Absolute Recovery

HupA standard solutions (sample 1) with low, medium and high concentrations (0.25, 5 and 80 ng/mL) were prepared with the mobile phase. The blank plasma samples of the mice were processed according to *Section sample preparation*, and the residual was redissolved with sample 1. After centrifugation, the supernatant was analyzed by LC-MS/MS (sample 2). QC samples with low, medium and high concentrations (0.25, 5 and 80 ng/mL) of HupA were prepared from the blank plasma of mice, processed according to *Section sample preparation* and determined by the LC-MS/MS method (sample 3). The ratio of the chromatographic peak area of sample 2to the chromatographic peak area of sample 1 was the matrix effect of plasma samples. The ratio of the chromatographic peak area of sample 3 to the chromatographic peak area of sample 2 was the absolute recovery rate of the plasma samples. The same method was used to calculate the absolute recovery rate based on brain tissue samples with low, medium and high concentrations of 0.25, 2.5, and 40 ng/mL, respectively.

Analyses of the Sample Stability

The stability of the HupA in the biological plasma samples was investigated. QC samples with low, medium and high concentrations (0.25, 5 and 80 ng/mL, respectively) of HupA were prepared from blank mouse plasma. The drug concentration in plasma was determined after repeated freezing-thawing at room temperature for 8 and 24 h and refrigerated at -20°C for 30 days. The

stability of the samples under different conditions and the influence of repeated freezing-thawing on the drug were investigated.

Compared with the initial value, the ratio of chromatographic peak area of the internal standard solution obtained after the above-described treatment was expressed as a percentage to indicate the stability of the sample.

Animal and Drug Administration

ICR mice weighing 20±2.0 g (half male and half female) were provided by Beijing Huafukang Biotechnology Co., Ltd. (Beijing, China). All the mice were housed in ideal laboratory conditions which had free access to food and fresh drinking water with an alternating lightdark cycle at constant temperatures. The animal experiment was carried out in compliance with the protocol of Animal Use and Care by State Key Laboratory of NBC Protection for Civilians. The ICR mice were randomly divided into the HupA control group, the 46.4-nm HupA-PLGA-NP group and the 208.5-nm HupA-PLGA-NP group. A dose (containing HupA) of 0.5 mg/kg was administered via the tail vein to all the mice. This study was approved by the Animal Ethics Committee of State Key Laboratory of NBC Protection for Civilian Animal Center.

Collection and Pretreatment of Plasma and Brain Tissue Samples

Blood samples were collected at different time points (0 min, 5 min, 15 min, 30 min, 1 h, 2 h, 4 h, 8 h, 12 h, and 24 h) after drug administration. Blood (0.5 ml) obtained from the heart was transferred to an Eppendorf tube with anticoagulant agent and then centrifuged at 5000 rpm for 10 min. The plasma was transferred to another Eppendorf tube at 4°C for analysis.

At the same time, the mice were sacrificed by surgical dislocation of the necks. Brain tissue samples were collected from an ice bath, and the remaining blood samples and large blood vessels on the tissue surface were washed with saline. The water was then removed with filter paper. The brain tissues were weighed and homogenized with saline at a ratio of 1:4. The homogenate was centrifuged at 10000 rpm for 10 min. The supernatant was transferred to an Eppendorf tube and then frozen at -20°C.

Determination of the HupA Content

The established LC-MS/MS method was used to determine the drug concentration of HupA in the blood and brain tissue samples.

Analyses of Pharmacokinetic Parameters

PKS pharmacokinetic software was used to fit the drug concentration in plasma and the brain over time. The area under the curve (AUC_{0-u}) was calculated by the trapezoidal method to analyze the pharmacokinetic parameters. The values of all experimental data are expressed as the means ± standard deviations ($\bar{X}$±SD).

Calculation of the Relative Bioavailability

The relative bioavailability of the different groups was calculated according to the following formula: $F=(AUC_T \times R \text{ dosage})/(AUC_R \times T \text{ dosage}) \times 100\%$, where T and R represent the HupA nanodrugs and HupA prototype drugs, respectively.

Brain-Targeted Evaluation

The drug targeting index (DTI) is an important indicator for evaluating the in vivo targeting of drugs after administration. First, the brain-targeted drug-targeting efficiency (DTE) of free drugs and nanodrugs was calculated according to the following formula: $DTE=AUC_{tissue}/AUC_{blood}$. The brain-targeted DTI of nanodrugs with different NP sizes relative to that of free drugs was calculated according to the following formula: brain-targeted $DTI=DTE_{(nanodrugs)}/DTE_{(free\ drugs)}$. If the DTI was equal to or close to 1, the brain-targeted efficiency of the two drugs was equivalent. If the DTI was markedly higher than 1, the brain-targeted efficiency of the nanodrugs was higher than that of free drugs.

Results

LC-MS/MS Detection of HupA in Biological Samples

Under the selected chromatographic conditions, HupA and the IS HupB mainly generated excimer $[M+H]^+$ ion peaks of m/z 243.1 and m/z 257.1, respectively. The $[M+H]^+$ peaks were selectively analyzed by full scanning analysis. The main debris ions generated by HupA and the IS HupB were m/z 226.1 and m/z 240.1, respectively, and these were used as the monitored product ions for the quantitative analysis. The two-level optimization program of the instrument was used for optimization. The final optimization collision energy was 18 eV. The primary and secondary mass spectra of HupA and the IS HupB are shown in Figure 1.

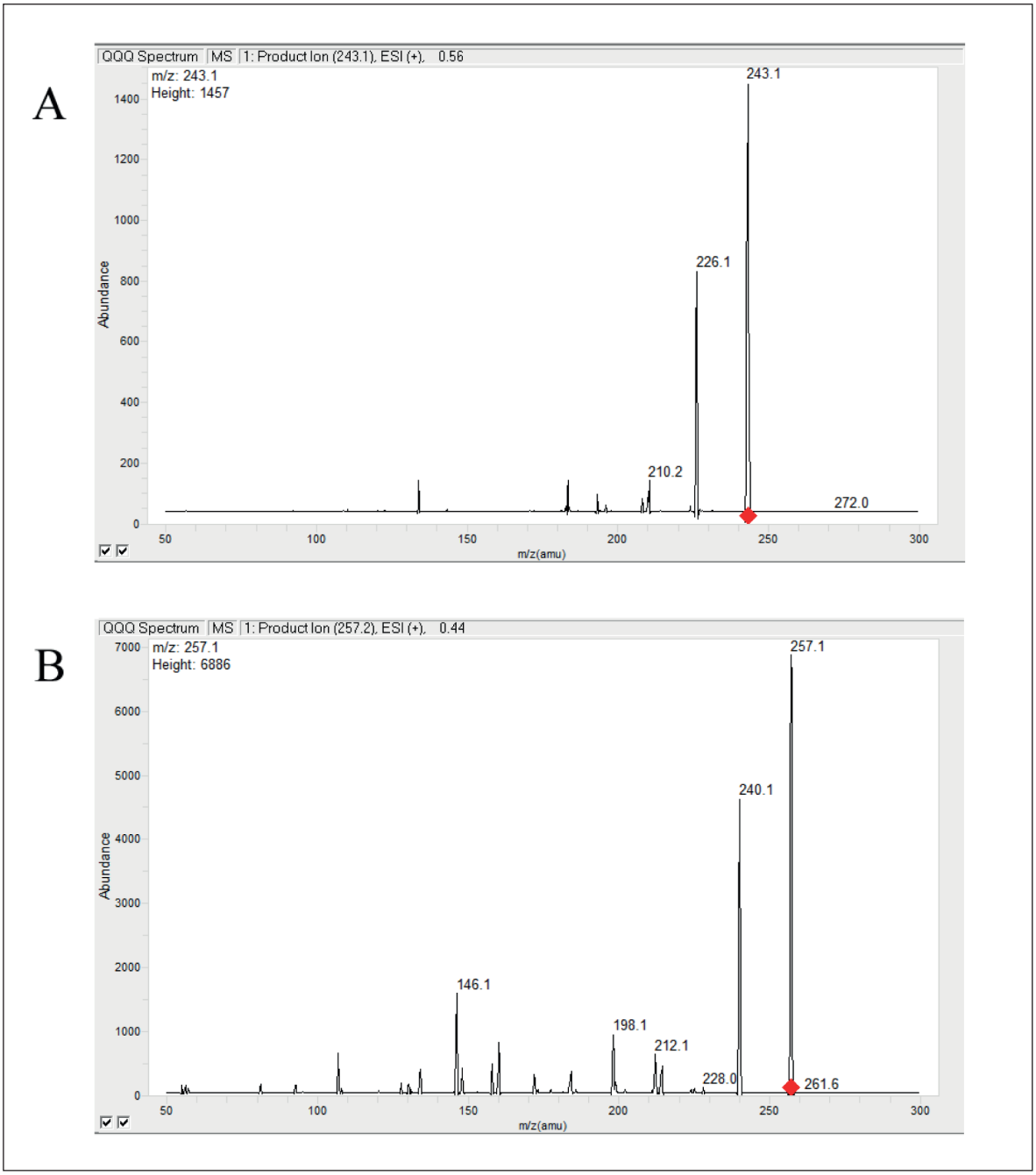

Figure 1. Primary and secondary mass spectra of HupA (**A**) and the internal standard HupB (**B**).

Specificity of the Method

The specificity of the method with the selected LC-MS/MS conditions was found to be good. The specific spectra of the plasma and brain tissue samples from mice are shown in Figures 2 and 3. The retention times of HupA and the IS HupB were 1.28 and 1.32 min, respectively. The endogenous substances in blank plasma and brain tissue showed no obvious interference with the determination of HupA and the IS HupB.

Linear Range and Lower Limit of Quantification

The concentration of HupA in the sample was taken as the abscissa, and the ratio of the peak area between HupA and the IS HupB was taken as the ordinate. Linear regression analyses were

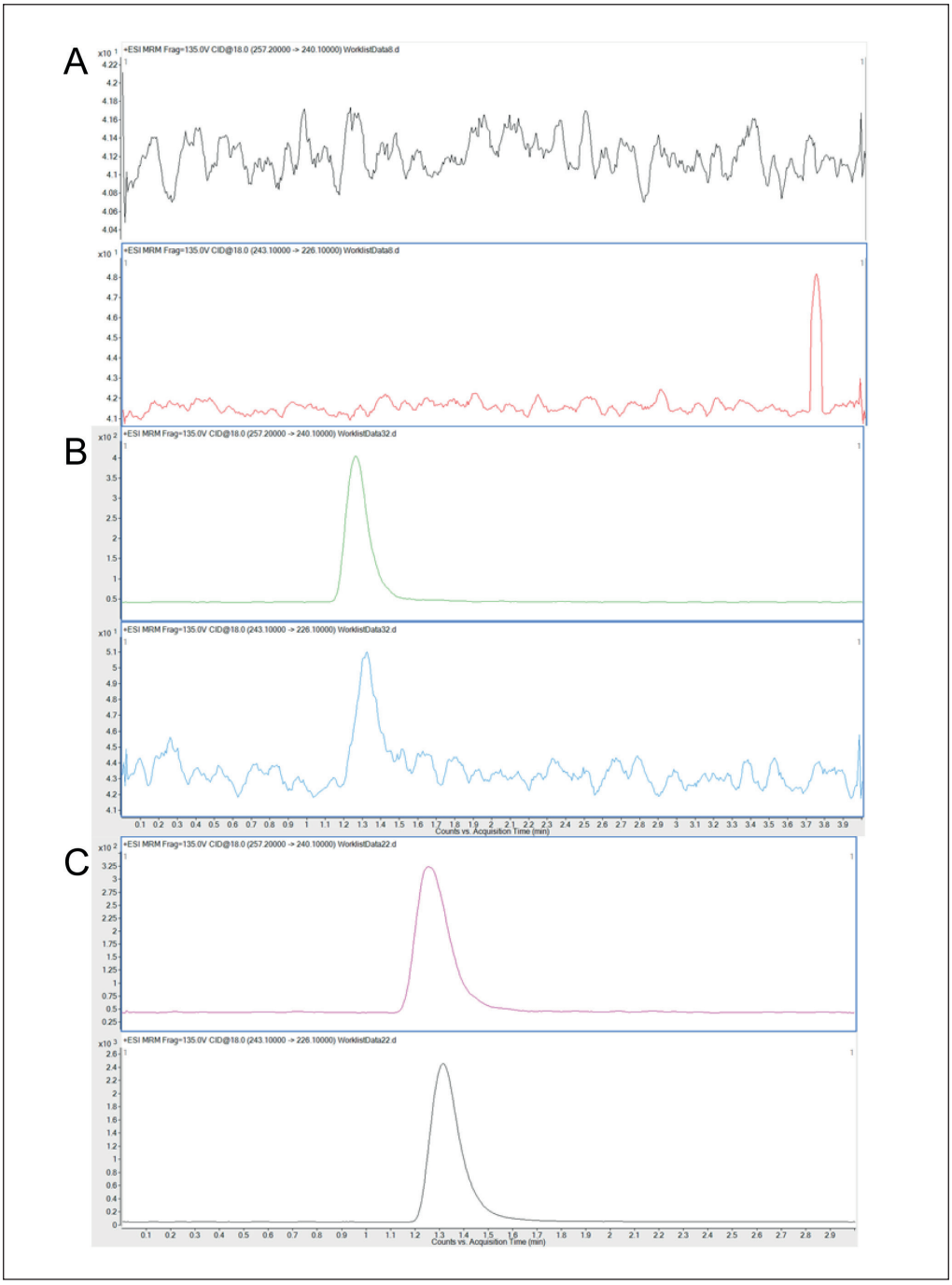

Figure 2. LC-MS/MS specificity of plasma samples. **A**, Blank plasma samples. **B**, Blank plasma samples with HupA (0.1 ng/mL) and HupB (5 ng/mL). **C**, Plasma samples obtained 15 min after drug administration.

conducted using the 1/y weighted least-square method. The standard curves of the plasma and brain tissue samples were y=0.0106+0.0995x (R^2=0.9988) and y=0.0089+0.1205x (R^2=0.9986), respectively. The plasma samples showed a good linear relationship in the range of 0.1 to 100 ng/mL, and the brain tissue samples showed a good linear relationship in the range of 0.1 to 50 ng/mL. The quantitative lower limit was investigated using a concentration of 0.1 ng/mL. The results showed that the relative recovery rates of the plasma and brain samples were 94.8% and 97.2%, respectively. Therefore, the lower limit of quantification was determined to equal 0.1 ng/mL.

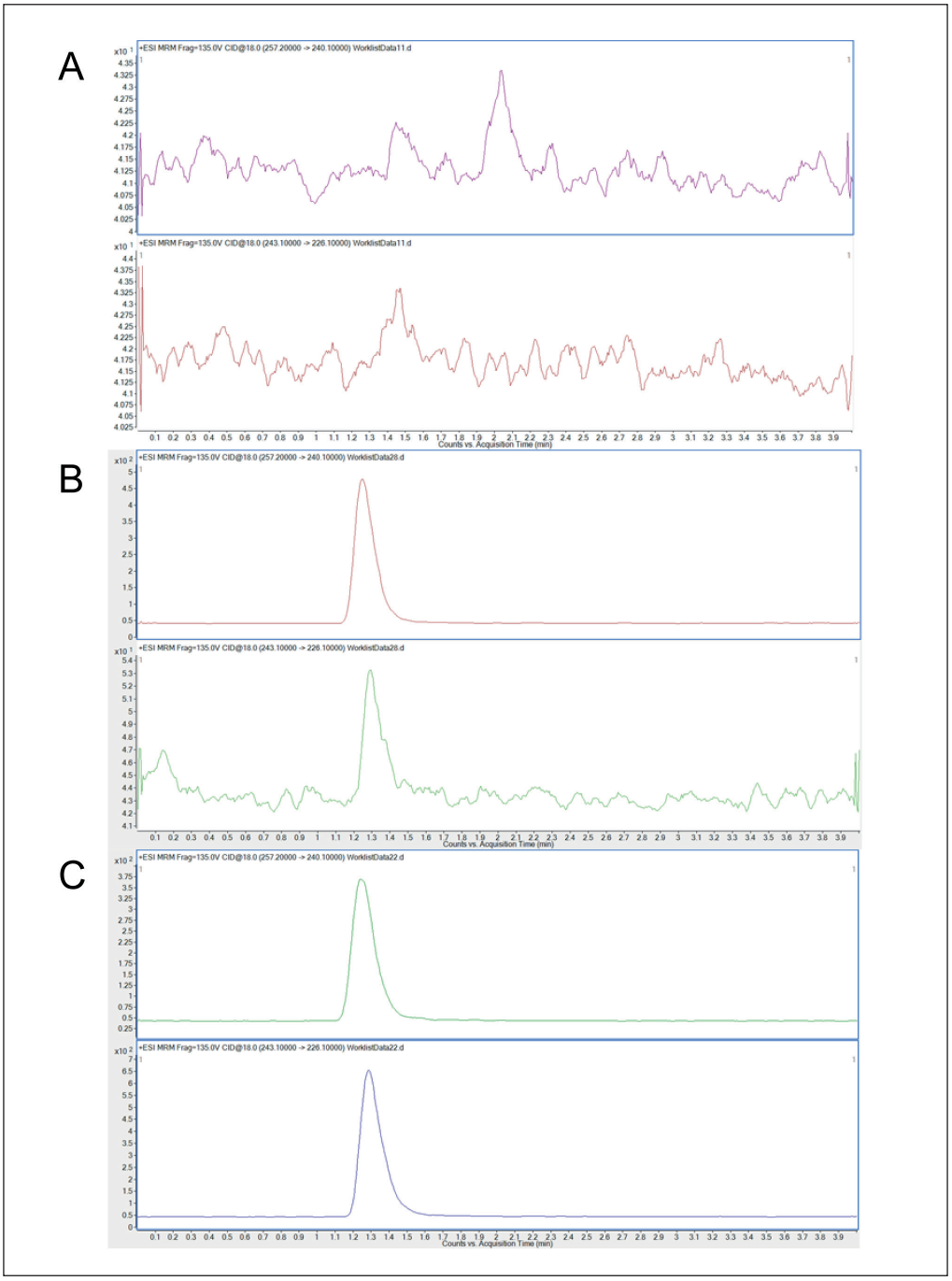

Figure 3. LC-MS/MS specificity of brain tissue samples. **A**, Blank brain samples. **B**, Blank brain samples with HupA (0.1 ng/mL) and HupB (5 ng/mL). **C**, Brain samples obtained 15 min after drug administration.

Inspection of the Precision and Accuracy

The results from the analysis of the precision and accuracy of the established LC-MS/MS method are shown in Table I. The intraday RSD of the plasma and brain tissue samples with standard samples at low, medium and high concentrations was between 1.77% and 12.74%. The diurnal RSD (for 5 consecutive days) was 0.80%-8.81%. The precision and accuracy of this method was found to meet the requirements of biological sample analysis.

Matrix Effects and Absolute Recovery

The matrix components in the samples inhibited the HupA and HupB signals to a certain ex-

Table I. Inspection of precision and accuracy of LC-MS/MS method.

Type	Concentration(ng/ml)	Intraday precision		Diurnal precision		Accuracy (%)
		$\bar{X}$±SD	RSD (%)	$\bar{X}$±SD	RSD (%)	
Plasma	0.25	0.26±0.01	4.85	0.24±0.02	8.81	-4.26
	5	4.93±0.34	6.88	5.17±0.19	3.68	+3.37
	80	79.01±3.10	3.92	77.83±2.95	3.80	-2.72
Brain	0.25	0.25±0.03	12.74	0.27±0.02	6.44	+6.31
	2.5	2.43±0.06	2.63	2.47±0.03	1.30	-1.00
	40	40.79±0.72	1.77	41.35±0.33	0.80	+3.38

tent, with inhibition rates ranging from 77.96% to 97.17% (Table II). However, the inhibition degrees obtained with the low, medium and high concentrations were basically the same, which indicated that it had little influence on the quantitative analysis of HupA and HupB.

The absolute recovery of HupA in the samples ranged from 72.41% to 87.43%, and that of HupB ranged from 78.15% to 79.25% (Table II). The absolute recovery had little influence on the sample determination and analysis.

Sample Stability

The results of the stability analysis of the plasma samples after incubation at room temperature for 8 h, storage at -20°C for one month, or subjected to three freeze-thaw cycles within 24 h are shown in Table III. The stability degree was in the range of 96.27% to 102.48%, and the RSD was in the range of 3.21% to 9.96%. The results showed that HupA was stable in plasma under the investigated conditions.

Stability of HupA-PLGA-NPs

HupA-PLGA-NP solution was prepared using the best preparation process. After the solution was incubated at room temperature for 15 days, no stratification or precipitation was observed in the solution, and the size and distribution of the NPs did not change. After 30 d, a small number of NPs agglomerated in the NP solution, and flocs were visible to the naked eye. No stratification or precipitation was observed in the solution, and the size and distribution of NPs did not change when the solution was placed in the refrigerator at 4°C for 3 months. The maintenance of the NPs in the refrigerator at 4°C for 6 months did not change the size and distribution of the NPs, as observed by TEM.

Relationship Between the Blood Concentration and Time in Plasma

HupA-PLGA-NPs (0.5 mg/kg) with sizes of 46.4 and 208.5 nm were injected into the mice by tail vein. The HupA concentration in plasma is shown in Table IV and Figure 4. The results from the analysis of pharmacokinetic parameters, which are shown in Table V, indicated that the C_{max} values obtained for the 46.4- and 208.5-nm HupA-PLGA-NPs were 156.64 and 160.13 ng/mL, respectively, which was almost equal to that of the HupA control (157.65 ng/mL). $T_{1/2}$ values of 6.20 and 7.90 h were obtained for the 46.4 and 208.5-nm HupA-PLGA-NPs, respectively, and these values were 1.5- and 2.0-fold longer than the $T_{1/2}$ of the HupA control, respectively (4.04 h). The MRT values for the 46.4- and 208.5-nm HupA-PLGA-NPs were 6.23 and 7.01 h, which were 2.9- and 3.3-fold longer than the MRT of the HupA control, respectively (2.14 h).

The relative bioavailability of HupA-PLGA-NPs was calculated according to the area under the drug concentration and time curve ($AUC_{0\text{-}24h}$), as shown in Table V. At a dose of 0.5 mg/kg, the relative bioavailabilities of the 46.4- and 208.5-nm HupA-PLGA-NPs were 1.93- and 2.19-fold higher than that of the HupA control, respectively.

Table II. Inspection of matrix effect and absolute recovery of plasma and brain tissue homogenates ($\bar{x}$±SD).

Type	Matrix effect of HupA(%)			Absolute recovery of HupA (%)			HupB (%)	
	Low	Medium	High	Low	Medium	High	Matrix effect	Absolute recovery
Plasma	86.95±10.57	81.09±1.16	80.14±1.52	73.60±11.88	72.41±8.56	87.43±5.34	80.74±4.80	78.51±5.69
Brain	77.96±7.90	89.62±6.67	97.17±2.33	83.29±7.52	85.53±9.65	76.12±4.22	86.70±2.23	79.25±3.29

Table III. The stability of HupA in plasma samples.

Time and conditions	Concentration (ng/mL)	Percentage of initial value (%)	RSD (%)
Room temperature for 8	0.25	100.29±5.81	5.78
	5	101.81±6.17	6.09
	80	99.76±3.24	3.21
-20°C for 30 d	0.25	96.27±5.51	5.71
	5	100.57±7.76	7.85
	80	98.38±5.36	5.49
Frozen and thawed for 3 times within 24 h	0.25	102.48±8.87	8.68
	5	101.37±10.08	9.96
	80	100.52±5.22	5.17

Relationship Between the Drug Concentration and Time in the Brain

The HupA concentration in the brain is shown in Table VI and Figure 5. The results from the analysis of the pharmacokinetic parameters, which are shown in Table VII, revealed that the C_{max} values of the 46.4- and 208.5-nm HupA-PLGA-NPs were 40.05 and 60.18 ng/mL, respectively; the former value was almost the same as the C_{max} of the HupA control (37.98 ng/mL), and the latter was approximately 1.6-fold higher than that of the HupA control. The T_{max} of the 46.4- and 208.5-nm HupA-PLGA-NPs was 1.25±0.61 h, which was approximately 2.5-fold longer than the T_{max} of the HupA control (0.5 h). The $T_{1/2}$ values of the 46.4- and 208.5-nm HupA-PLGA-NPs were 12.53 and 8.47 h, respectively, which were 1.82- and 1.23-fold longer than that of the HupA control (6.89 h). The MRTs of the 46.4- and 208.5-nm HupA-PLGA-NPs were 16.59 and 7.04 h, respectively; the former value was 2.26-fold longer than the MRT of the HupA control (7.34 h), and the latter was almost the same as that of the HupA control.

Brain Targeting Evaluation

The brain-targeted DTEs of the HupA control and the 46.4- and 208.5-nm HupA-PLGA-NPs were 0.81, 1.20, and 0.66, respectively, and the DTIs of the 46.4- and 208.5-nm HupA-PLGA-NPs were 1.48 and 0.81, respectively.

Discussion

The LC-MS/MS method established in our study had the advantages of good specificity, high sensitivity, needing a low sample among and low economic cost, which makes it particularly suitable for determination of the drug content in plasma and brain samples.

Nanomaterials are one of the most promising formulations in targeted drug delivery systems. It has been reported that the oral bioavailabilities of polyene paclitaxel phospholipid NPs and honokiol self-emulsion were 3.65- and 1.33-fold higher than that of the control group[13,14]. In addition, the bioavailability of bufalin albumin NPs was between 1.19- and 1.81-fold higher than that of the control group,

Table IV. Drug concentration in plasma of mice.

Time(h)	HupA control		46.4 nm HupA-PLGA-NPs		208.5 nm HupA-PLGA-NPs	
	$\bar{X}$	SD	$\bar{X}$	SD	$\bar{X}$	SD
0.08	157.65	13.85	156.64	19.53	160.13	11.87
0.25	114.79	13.72	125.14	17.45	134.19	14.41
0.5	76.84	10.22	83.28	13.67	108.72	7.41
1	44.30	8.41	54.74	9.44	75.34	12.58
2	27.98	5.90	39.62	7.81	44.08	8.28
4	7.25	0.87	21.76	9.64	25.54	5.26
8	1.80	0.30	13.04	5.02	12.72	2.83
12	0.50	0.08	6.21	2.53	6.24	1.71
24	0.24	0.07	2.19	0.78	2.91	0.41

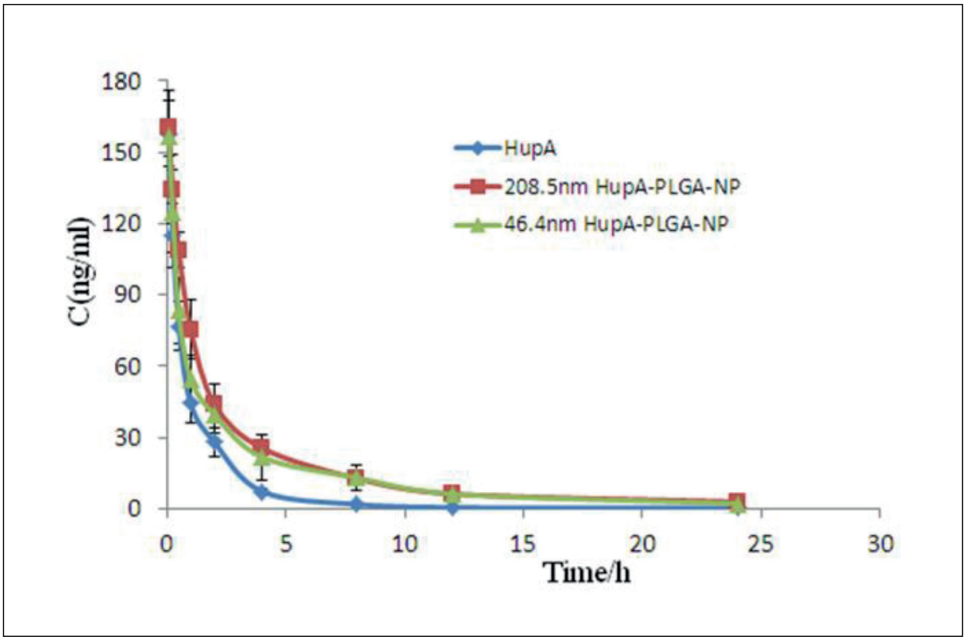

Figure 4. Curve of the drug concentration in plasma.

and the half-life was between 2.17- and 2.94-fold higher than that of the control group[15]. The results obtained in our study showed that the half-lives of the 46.4- and 208.5-nm HupA-PLGA-NPs in blood were 6.20 and 7.90 h, which are 1.53- and 1.96-fold higher than the half-life of the HupA control (4.04 h), respectively, and this finding is consistent with the results of the in vitro release of HupA-PLGA-NPs with different sizes[12]. These findings might be attributed to the rapid release of drugs adsorbed on the surface of nanoparticles with small sizes[16-18]. The MRTs of the 46.4- and 208.5-nm HupA-PLGA-NPs were 6.23 and 7.01 h, which are 2.9- and 3.3-fold longer than that of the HupA control, respectively. The results indicate that HupA-PLGA-NPs with different sizes have better sustained release effects and significantly extend the in vivo action time of drugs. These findings are consistent with those obtained with other novel preparations of HupA, such as HupA-polylactic acid (PLA)-microspheres and HupA microemulsion in situ gel for nasal delivery[19,20]. Additionally, the bioavailability of the two groups were 1.93- and 2.19-fold higher than that of the HupA control, respectively. This result was consistent with hat obtained in another study[21], which found that the concentration and retention time of drugs in plasma increased significantly after drug nanorization. In summary, HupA nanorization improves the half-life and bioavailability of HupA. Moreover, the NP characteristics and drug properties can influence the in vivo distribution patterns in certain ways.

The BB permeability has been found to be a size-dependent property by comparing the BBB

Table V. Different pharmacokinetic parameters in plasma.

Parameter	HupA Control	46.4 nm-HupA-PLGA-NPs	208.5 nm-HupA-PLGA-NPs
C_{max} (ng/mL)	157.65±13.85	156.64±19.53	160.13±11.87
T_{max} (h)	0.08±0.00	0.08±0.00	0.08±0.00
$T_{1/2}$ (h)	4.04±0.68	6.20±0.84	7.90±1.21
AUC_{0-24h}	188.51±20.72	364.10±88.91	412.87±47.79
$AUC_{0-\infty}$	189.86±20.73	383.70±93.53	445.69±46.79
MRT (h)	2.14±0.11	6.23±0.84	7.01±0.69

Table IV. Drug content in brain tissue of mice (ng/mL).

Time(h)	HupA control		46.4 nm-HupA-PLGA-NPs		208.5 nm-HupA-PLGA -NPs	
	$\bar{X}$	SD	$\bar{X}$	SD	$\bar{X}$	SD
0.08	17.93	3.54	23.44	3.20	32.75	8.48
0.25	25.89	7.67	29.23	2.64	44.38	6.91
0.5	37.98	5.80	32.60	9.50	48.65	8.37
1	28.23	5.04	33.47	7.20	55.35	5.85
2	19.33	5.12	35.87	7.94	50.44	7.49
4	8.79	2.76	21.71	7.44	18.58	5.61
8	4.80	2.24	15.30	4.25	7.26	2.53
12	2.02	0.72	10.21	3.02	3.06	0.45
24	1.21	0.16	6.51	1.72	1.88	0.61

permeabilities of NPs[22,23]. Based on the results from the analysis of the HupA concentration in the brain, we found that the T_{max}, $T_{1/2}$, and MRT of the 46.4-nm HupA-PLGA-NPs, and the C_{max}, T_{max}, and $T_{1/2}$ of the 208.5-nm HupA-PLGA-NPs were all higher than the corresponding values found for the HupA control. These findings indicate that nanodrugs exert obvious sustained release effects in the brain, and the removal of the 46.4-nm HupA-PLGA-NPs was found to be slower than that of the 208.5-nm HupA-PLGA-NPs, which was consistent with the distribution patterns of 50-nm DiR-PLGA-NPs[24]. Moreover, the DTIs of the 46.4- and 208.5-nm HupA-PLGA-NPs were 1.48 and 0.81, respectively, which suggested that the 46.4-nm HupA-PLGA-NPs exhibit obvious brain targeting, whereas the 208.5-nm HupA-PLGA-NPs showed no obvious brain targeting. This finding was consistent with the dynamic distribution patterns of tracer NPs of different sizes in mice. These results suggest that the NP size is associated with the tissue distribution patterns of nanodrugs. Therefore, a particular NP size can be selected to maximize the pharmacodynamic effects and control the toxicity of nanodrugs.

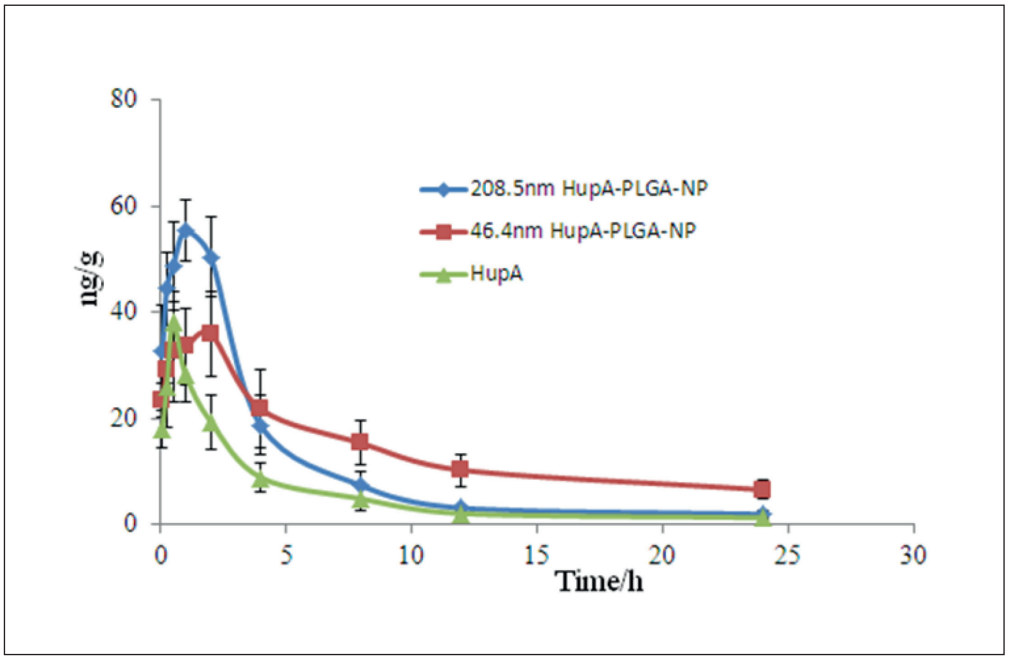

Figure 5. Curve of the drug concentration in the brain.

Table VII. Different pharmacokinetic parameters in brain tissue of mice.

Parameter	HupA Control	46.4 nm-HupA-PLGA-NPs	208.5 nm-HupA-PLGA-NPs
C_{max} (ng/ml)	37.98±5.80	40.05±6.79	60.18±2.81
T_{max} (h)	0.50±0.00	1.25±0.61	1.25±0.61
$T_{1/2}$ (h)	6.89±1.42	12.53±2.44	8.47±1.81
AUC_{0-24h}	141.82±36.95	348.17±75.32	270.64±14.82
$AUC_{0-\infty}$	153.80±36.96	461.31±85.90	293.97±19.93
MRT (h)	7.34±0.68	16.59±1.96	7.04±1.25

Conclusions

In summary, the LC-MS/MS method established in this study has the advantages of good specificity, high sensitivity, needing a low sample among and a low economic cost, which makes it particularly suitable for determination of the drug content in plasma and brain samples. HupA nanorization exerted significant effects on pharmacokinetic parameters and increased the half-life and bioavailability of drugs. The 46.4-nm HupA-PLGA-NPs presented obvious brain targeting, whereas the 208.5-nm HupA-PLGA-NPs showed no evident brain targeting. These results suggest that the NP size is associated with the tissue distribution patterns of nanodrugs. Therefore, a particular NP size can be selected to maximize the pharmacodynamic effects and control the toxicity of nanodrugs.

Conflict of Interest

The authors declared no conflict of interest.

References

1) Ma X, Gang DR. In vitro production of huperzine A, a promising drug candidate for Alzheimer's disease. Phytochemistry 2008; 69: 2022-2028.
2) Agatonovic-Kustrin S, Kettle C, Morton DW. A molecular approach in drug development for Alzheimer's disease. Biomed Pharmacother 2018; 106: 553-565.
3) Little JT, Walsh S, Aisen PS. An update on huperzine A as a treatment for Alzheimer's disease. Expert Opin Investig Drugs 2008; 17: 209-215.
4) Tsai SJ. Huperzine-A, a versatile herb, for the treatment of Alzheimer's disease. J Chin Med Assoc 2019; 82: 750-751.
5) Dunnhaupt S, Kammona O, Waldner C, Kiparissides C, Bernkop-Schnurch A. Nano-carrier systems: Strategies to overcome the mucus gel barrier. Eur J Pharm Biopharm 2015; 96: 447-453.
6) Meng Q, Wang A, Hua H, Jiang Y, Wang Y, Mu H, Wu Z, Sun K. Intranasal delivery of Huperzine A to the brain using lactoferrin-conjugated N-trimethylated chitosan surface-modified PLGA nanoparticles for treatment of Alzheimer's disease. Int J Nanomedicine 2018; 13: 705-718.
7) Yang CR, Zhao XL, Hu HY, Li KX, Sun X, Li L, Chen DW. Preparation, optimization and characteristic of huperzine a loaded nanostructured lipid carriers. Chem Pharm Bull (Tokyo) 2010; 58: 656-661.
8) Wohlfart S, Gelperina S, Kreuter J. Transport of drugs across the blood-brain barrier by nanoparticles. J Control Release 2012; 161: 264-273.
9) Jiang Y, Huo S, Mizuhara T, Das R, Lee YW, Hou S, Moyano DF, Duncan B, Liang XJ, Rotello VM. The Interplay of Size and Surface Functionality on the Cellular Uptake of Sub-10 nm Gold Nanoparticles. Acs Nano 2015; 9: 9986-9993.
10) Lu F, Wu SH, Hung Y, Mou CY. Size effect on cell uptake in well-suspended, uniform mesoporous silica nanoparticles. Small 2009; 5: 1408-1413.
11) Jiang W, Kim BY, Rutka JT, Chan WC. Nanoparticle-mediated cellular response is size-dependent. Nat Nanotechnol 2008; 3: 145-150.
12) Wang HY, Wu M, Diao JL, Li JB, Sun YX, Xiao XQ. Huperzine A ameliorates obesity-related cognitive performance impairments involving neuronal insulin signaling pathway in mice. Acta Pharmacol Sin 2020; 41: 145-153.
13) Hou J, Sun E, Sun C, Wang J, Yang L, Jia XB, Zhang ZH. Improved oral bioavailability and anticancer efficacy on breast cancer of paclitaxel via Novel Soluplus((R))-Solutol((R)) HS15 binary mixed micelles system. Int J Pharm 2016; 512: 186-193.
14) Wan L, Wang X, Zhu W, Zhang C, Song A, Sun C, Jiang T, Wang S. Folate-polyethyleneimine functionalized mesoporous carbon nanoparticles for enhancing oral bioavailability of paclitaxel. Int J Pharm 2015; 484: 207-217.
15) Zhang HQ, Yin ZF, Sheng JY, Jiang ZQ, Wu BY, Su YH. [A comparison study of pharmacokinetics between bufalin-loaded bovine serum albumin nanoparticles and bufalin in rats]. Zhong Xi Yi Jie He Xue Bao 2012; 10: 674-680.

16) Chu DF, Fu XQ, Liu WH, Liu K, Li YX. Pharmacokinetics and in vitro and in vivo correlation of huperzine A loaded poly(lactic-co-glycolic acid) microspheres in dogs. Int J Pharm 2006; 325: 116-123.

17) Fu XD, Gao YL, Ping QN, Ren T. Preparation and in vivo evaluation of huperzine A-loaded PLGA microspheres. Arch Pharm Res 2005; 28: 1092-1096.

18) Fu X, Ping Q, Gao Y. Effects of formulation factors on encapsulation efficiency and release behaviour in vitro of huperzine A-PLGA microspheres. J Microencapsul 2005; 22: 57-66.

19) Gao P, Ding P, Xu H, Yuan Z, Chen D, Wei J, Chen D. In vitro and in vivo characterization of huperzine a loaded microspheres made from end-group uncapped poly(d,l-lactide acid) and poly(d,l-lactide-co-glycolide acid). Chem Pharm Bull (Tokyo) 2006; 54: 89-93.

20) Chen Y, Cheng G, Hu R, Chen S, Lu W, Gao S, Xia H, Wang B, Sun C, Nie X, Shen Q, Fang W. A Nasal Temperature and pH Dual-Responsive In Situ Gel Delivery System Based on Microemulsion of Huperzine A: Formulation, Evaluation, and In Vivo Pharmacokinetic Study. Aaps Pharmscitech 2019; 20: 301.

21) Chu KS, Hasan W, Rawal S, Walsh MD, Enlow EM, Luft JC, Bridges AS, Kuijer JL, Napier ME, Zamboni WC, DeSimone JM. Plasma, tumor and tissue pharmacokinetics of Docetaxel delivered via nanoparticles of different sizes and shapes in mice bearing SKOV-3 human ovarian carcinoma xenograft. Nanomedicine-Uk 2013; 9: 686-693.

22) Hanada S, Fujioka K, Inoue Y, Kanaya F, Manome Y, Yamamoto K. Cell-based in vitro blood-brain barrier model can rapidly evaluate nanoparticles' brain permeability in association with particle size and surface modification. Int J Mol Sci 2014; 15: 1812-1825.

23) Cai X, Bandla A, Mao D, Feng G, Qin W, Liao LD, Thakor N, Tang BZ, Liu B. Biocompatible Red Fluorescent Organic Nanoparticles with Tunable Size and Aggregation-Induced Emission for Evaluation of Blood-Brain Barrier Damage. Adv Mater 2016; 28: 8760-8765.

24) Wen Z, Yan Z, He R, Pang Z, Guo L, Qian Y, Jiang X, Fang L. Brain targeting and toxicity study of odorranalectin-conjugated nanoparticles following intranasal administration. Drug Deliv 2011; 18: 555-561.